Environ Geol (2009) 57:483–497
DOI 10.1007/s00254-008-1318-9

ORIGINAL ARTICLE

Soil erosion prediction using the Revised Universal Soil Loss Equation (RUSLE) in a GIS framework, Chania, Northwestern Crete, Greece

Maria Kouli · Pantelis Soupios · Filippos Vallianatos

Received: 24 September 2007 / Accepted: 3 April 2008 / Published online: 26 April 2008

Abstract Soil erosion is a growing problem in southern Greece and particularly in the island of Crete, the biggest Greek island with great agricultural activity. Soil erosion not only decreases agricultural productivity, but also reduces the water availability. In the current study, an effort to predict potential annual soil loss has been conducted. For the prediction, the Revised Universal Soil Loss Equation (RUSLE) has been adopted in a Geographical Information System framework. The RUSLE factors were calculated (in the form of raster layers) for the nine major watersheds which cover the northern part of the Chania Prefecture. The *R*-factor was calculated from monthly and annual precipitation data. The *K*-factor was estimated using soil maps available from the Soil Geographical Data Base of Europe at a scale of 1:1,000,000. The *LS*-factor was calculated from a 30-m digital elevation model. The *C*-factor was calculated using Remote Sensing techniques. The *P*-factor in absence of data was set to 1. The results show that an extended part of the area is undergoing severe erosion. The mean annual soil loss is predicted up to $\sim$200 (t/ha year^{-1}) for some watersheds showing extended erosion and demanding the attention of local administrators.

Keywords Soil erosion · RUSLE · GIS · Remote sensing · Western Crete

M. Kouli (✉) · P. Soupios · F. Vallianatos
Institute of Natural Resources and Natural Hazards, Center of Technological Research of Crete (CTRC), 3 Romanou, Chalepa, 73133 Chania, Crete, Greece
e-mail: mkouli@chania.teicrete.gr

Introduction

Soil erosion is a natural process in which earth materials are entrained and transported across a given surface. It is regarded as the major and most widespread kind of soil degradation and as such, affects significantly the sustainable agricultural land use. Soil can be eroded mainly by wind and water. High winds can blow away loose soils from flat or hilly terrain, while erosion due to the energy of water occurs when water falls toward the earth and flows over the surface.

Other problems caused by soil erosion include loss of soil nutrients, declining crop yields, reduction in soil productivity (Renard et al. 1997). Moreover, soil moved by erosion carries nutrients, pesticides and other harmful farm chemicals into rivers, streams, and ground water resources (Nyakatawa et al. 2001) and as a result, protecting soils from erosion is important to sustain human life. Finally, soil erosion causes air pollution through emissions of radioactive gases such as carbon dioxide (CO_2), methane (CH_4), and nitrous oxide (N_2O) (Lal 2001; Boyle 2002).

Accelerated soil erosion is a serious problem worldwide, with inestimable economic and environmental impacts because of its extent, magnitude, rate, and complex processes (Lal 1994). Numerous human-induced activities, such as mining, construction, and agricultural activities, disturb land surfaces, resulting in erosion. Soil erosion from cultivated areas is typically higher than that from uncultivated areas (Brown 1984). Soil erosion can pose a great concern to the environment because cultivated areas can act as a pathway for transporting nutrients, especially phosphorus attached to sediment particles of river systems (Ouyang and Bartholic 1997).

The Council of Europe provides an overview of the extent of soil degradation in Europe (as a technical report)

using revised GLASOD data (Oldeman et al. 1991; Van Lynden 1995). The most dominant effect is the loss of topsoil, which in many cases is potentially very damaging. The most important physical factors in the process of soil erosion are climate, topography, and soil characteristics. Southern Europe and particularly the Mediterranean region is extremely prone to erosion as it suffers from long dry periods followed by heavy erosive rainfall, falling on steep slopes with fragile soils, resulting in considerable amounts of erosion (Onori et al. 2006).

In some parts of the Mediterranean region, erosion has reached a stage of irreversibility while in some places there is no more soil left. With a slow rate of soil formation, any soil loss of more than 1 t/ha year^{-1} can be considered as irreversible within a time span of 50–100 years. Losses of 20 to 40 t/ha in individual storms (that may happen once every two or three years) are measured regularly in Europe with losses of more than 100 t/ha measured in extreme events (Morgan 1992). In Greece, soil erosion affects 3.5 million hectares and thereby experiencing a situation amounting to 26.5% of the country's total land area (Mitsios et al. 1995).

Various approaches and equations for risk assessment or predictive evaluation on soil erosion by water are available in international literature. Wischmeier and Smith (1965, 1978) by collecting soil erosion data of 8,000 communities of 36 regions in 21 states in USA, analyzed and assessed various dominating factors of soil erosion, and introduced the universal soil loss equation (USLE) to assess soil erosion by water. Basically, USLE predicts the long-term average annual rate of erosion on a field slope based on rainfall pattern, soil type, topography, crop system, and management practices (soil erosion factors). For the past 15 years, more comprehensive research on soil erosion by water has been conducted. By including additional data and incorporating recent research results, the USLE methodology is improved and a revised version of this model (RUSLE) further enhanced its capability to predict water erosion by integrating new information made available through research of the past 40 years (Renard and Freimund 1994; Renard et al. 1997; Yoder and Lown 1995).

Moreover, the combined use of GIS and erosion models, such as USLE/RUSLE, has been proved to be an effective approach for estimating the magnitude and spatial distribution of erosion (Cox and Madramootoo 1998; Erdogan et al. 2007; Fernandez et al. 2003; Fu et al. 2006; Gong 2001; Lewis et al. 2005; Lim et al. 2005; Millward and Mersey 1999; Mitasova et al. 1996; Molnar and Julien 1998; Wu and Dong 2001; Wu and Wang 2007; Yitayew et al. 1999).

The goal of this research was the implementation of the RUSLE model in nine water basins of the northwestern Crete Island to estimate the soil loss in a Mediterranean region which is particularly prone to erosion processes. The applicability and the efficiency of the GIS and remote sensing methods for soil loss estimation are also presented.

Study site

Crete is considered a semi-arid region. The average annual precipitation is estimated to be 900 mm (Chartzoulakis et al. 2001). The study area is situated at latitudes between 35.32 and 35.54 and longitudes between 23.60 and 24.16 decimal degrees, in the western Crete Island and specifically in the northern part of Chania Prefecture. It comprises nine watersheds; the Magagistra, Kastelli, Milias, Tiflos, Arapi, Tavronitis, Keritis, Therissos, and Kalami watersheds from west to east as shown in Fig. 1. Some general geometrical characteristics of the studied watersheds are also given in Table 1.

The climate is sub-humid Mediterranean with humid and relatively cold winters and dry and warm summers. The annual rainfall for the broader area has been estimated to be 665 mm. It is estimated that from the total yearly precipitation on the plains about 65% is lost to evapotranspiration, 21% run off to sea and only 14% goes to recharging the groundwater (Chartzoulakis et al. 2001). The drought period extends over more than 6 months (May to October) with evaporation values ranging from 140 mm to more than 310 mm in the peak month (Tsagarakis et al. 2004).

Regarding the geological setting, the water basins lie in an area which is mainly composed of Quaternary deposits that form depositional plains oriented southwards, while Miocene to Pliocene sediments are widespread all over the study area. Dissected hills of phyllites and quartzites, a Late Carboniferous to Late Triassic package of sedimentary rocks composed mostly of quartz-rich siliciclastic sediments, with minor limestone, gypsum, and volcanic rocks (Krahl et al. 1983) are observed mainly in the central part of the study area. Late Triasic carbonates (Tripolis nappe) and Triassic to Early Cretaceous carbonates of the Trypalion nappe are also exposed in several parts of the study area. The geological formations are classified into four hydrolithological units: high permeability rocks which comprise the karstic limestones of Tripolis and Trypalion nappes, medium permeability rocks which consist of the Quaternary deposits as well as the Miocene to Pliocene conglomerates and marly limestones, low permeability rocks which consists of the Pliocene to Miocene marles and impervious rocks which consist of the phyllites–quartzites unit.

Finally, the land use of the study area is mainly agricultural (up to 80%), pasture coverage is up to 10% while the natural vegetation coverage represents less than the 10%.

All the aforementioned conditions constitute the study area particularly sensitive to extended soil washout in case of intense rainfall events.

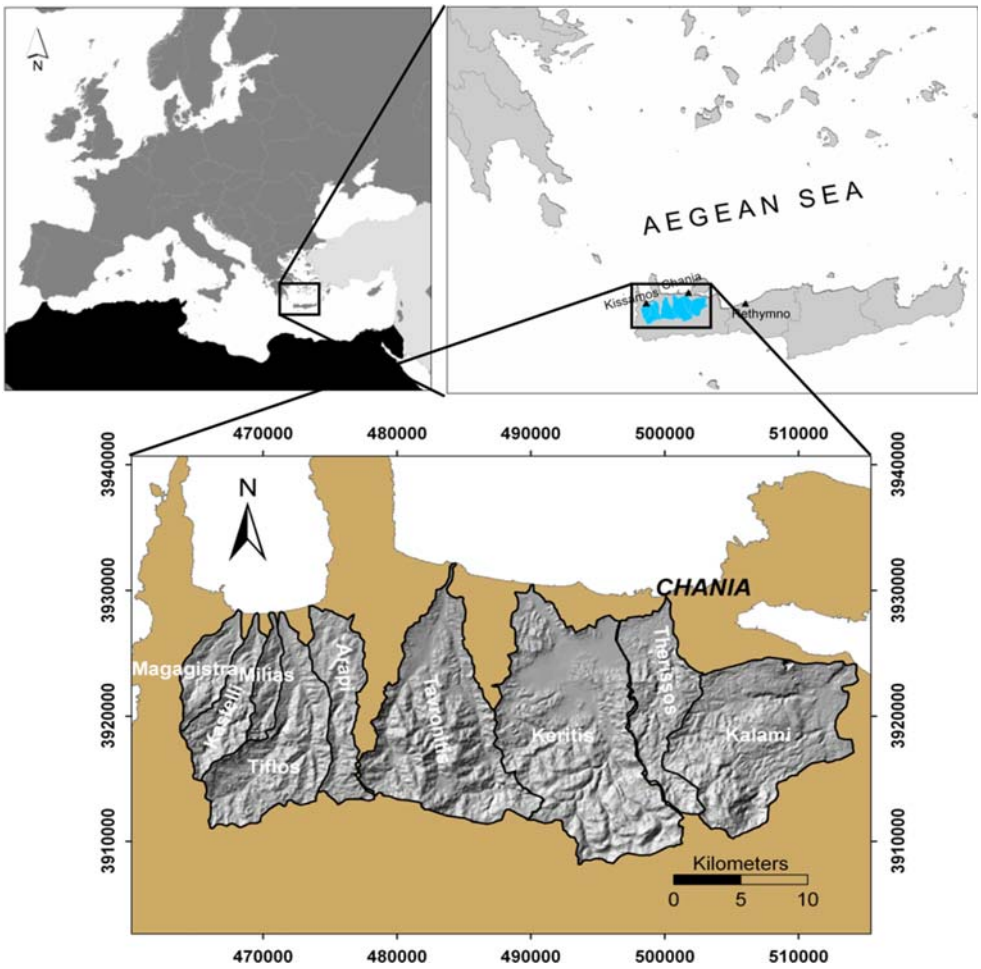

Fig. 1 Location maps of the studied watersheds

Table 1 Morphological characteristics of the studied watersheds

Watersheds	Minimum elevation	Maximum elevation	Area (km^2)	Perimeter (km)
Magagistra	20	923	22.53	24.07
Kastelli	20	1,061	31.70	32.86
Milias	20	816	15.35	23.94
Tiflos	20	1,163	76.07	48.36
Arapi	17	940	41.51	42.04
Tavronitis	0	1,295	130.86	63.51
Keritis	0	2,106	180.62	72.79
Therissos	11	2,078	57.46	47.70
Kalami	4	2,191	129.62	52.44

Materials and methods

Soil erosion prediction by RUSLE

Revised Universal Soil Loss Equation (RUSLE, Renard et al. 1997) is an empirically based model founded on the Universal Soil Loss Equation, USLE (Wischmeier and Smith 1978). RUSLE model enables prediction of an average annual rate of soil erosion for a site of interest for any number of scenarios involving cropping systems, management techniques, and erosion control practices. In the application of RUSLE on GIS environment, soil loss is estimated within the raster/grid GIS. Raster models are cell-based representations of map features, which offer analytical capabilities for continuous data and allow fast processing of map layer overlay operations (Fernandez et al. 2003).

Five major factors (rainfall pattern, soil type, topography, crop system, and management practices) are used in USLE/RUSLE for computing the expected average annual erosion through the following equation (Renard et al. 1997):

$$A = R \times K \times L \times S \times C \times P \quad (1)$$

where A is the computed spatial average soil loss and temporal average soil loss per unit area (t/ha $year^{-1}$), R the rainfall-runoff erosivity factor [MJ mm/(ha h $year^{-1}$)], K the soil erodibility factor [t ha h/(ha MJ mm)], L the slope-length factor, S the slope steepness factor, C the cover

management factor, and P the conservation support practice factor. L, S, C, and P are all dimensionless.

Data

The overall methodology involved use of RUSLE in a GIS environment. Individual GIS files were created for each factor in the RUSLE and combined by cell-grid modeling to predict soil loss in a spatial domain.

The following paragraphs describe the estimation of the R, K, C and LS factors from precipitation data, available geological and soil maps, digital processing of satellite images, and digital elevation model (DEM), respectively.

The P factor is the ratio of soil loss with a specific support practice to the corresponding loss with upslope–downslope tillage. These practices principally affect erosion by modifying the flow pattern, grade, or direction of surface runoff and by reducing the amount and rate of runoff (Renard and Foster 1983). Current agricultural practices observed in the northern part of Chania Prefecture consist of upslope–downslope tillage without any significant contouring or terracing. In order to remove/avoid the P factor from the soil loss estimation, P equal to 1 was assumed.

Rainfall erosivity factor (R)

Rainfall erosivity is defined as the aggressiveness of the rain to cause erosion (Lal 1990). The most common rainfall erosivity index is the R factor of USLE (Wischmeier and Smith 1965, 1978) and RUSLE (Renard et al. 1996). The R factor is considered to be the most highly correlated index to soil loss at many sites throughout the world (Aronica and Ferro 1997; Bergsma 1980; Bolinne et al. 1980; Ferro et al. 1991; Hussein 1986; Lo et al. 1985; Mikhailova et al. 1997; Renard and Freimund 1994; Stocking and Elwell 1973; Wischmeier 1959; Wischmeier and Smith 1978; Yu and Rosewell 1996a, b). The R factor for any given period is obtained by summing for each rainstorm—the product of total storm energy (E) and the maximum 30-min intensity (I_{30}). Since pluviograph and detailed rainstorm data are rarely available at standard meteorological stations, mean annual (Banasik and Gôrski 1994; Renard and Freimund 1994; Yu and Rosewell 1996c) and monthly rainfall amount (Ferro et al. 1991) have often been used to estimate the R factor for the USLE.

In an effort to estimate the R factor using monthly and annual rainfall data, Renard and Freimund (1994) proposed the use of both mean annual rainfall depth P and the previously introduced by Arnoldus (1980) modified Fournier index, F, which is defined as:

$$F = \sum_{i=1}^{12} \frac{p_i^2}{P} \tag{2}$$

where p_i, is the mean rainfall amount in mm for month i.

According to Arnoldus (1980) the F index is a good approximation of R to which it is linearly correlated. Moreover, by using mean annual rainfall data for different European regions (Bergsma 1980; Bolinne et al. 1980; Gabriels et al. 1986). Bagarello (1994) showed that the F index is strongly linearly correlated to the mean annual rainfall even in the case of seasonal variations in precipitation.

The F_F index which is well correlated with the rainfall erosivity (Ferro et al. 1991) was adopted to take into account the actual monthly rainfall distribution during each year ($F_{a,j}$) for a period of N years:

$$F_F = \sum_{j=1}^{N} \frac{F_{a,j}}{N} = \frac{1}{N} \sum_{j=1}^{N} \sum_{i=1}^{12} \frac{p_{i,j}^2}{P_j} \tag{3}$$

where p_{ij} is the rainfall depth in month/(mm) of the year j and P is the rainfall total for the same year.

Thus, the analysis of the erosivity factor using the aforementioned F_F index was carried out using data from 35 monthly recording rain-gauges. During the analysis, the R was found to be linearly and better correlated to F_F than P. This is in a good agreement with the results of Aronica and Ferro (1997). For regions, such as western Crete, where intensity indices (Ferro et al. 1991) are required for soil erosion studies, F_F is a better estimator of the R factor as it takes into account the rainfall seasonal distribution, while P is a robust estimator in regions where high rainfall erosivity corresponds to high annual rainfall.

Table 2 lists the individual data sets and indicates the name of the station, longitude/latitude and elevation of the station, the length of records in years, the network where the station belongs and some calculated parameters which will be commented in later section. The spatial distribution of the rain-gauge stations is shown in Fig. 2. For our research, data obtained from three different agencies: the Department of Hydrology of the Ministry of Agriculture and Development Organization of Western Crete (DHMA), the National Agricultural Research Foundation located in Chania in Crete Island (NAGREF), and the Institute of Geology and Mineral Exploration (IGME) (Branch of Crete).

The data sets obtained from the aforementioned data centers exhibit variable quality status. In order to exclude the most obvious errors from the precipitation data set in the study area, a quality control procedure was applied to all the monthly observations prior to their spatial analysis.

Table 2 Characteristics of the Western Crete rain-gauge stations used to derive the rainfall erosivity factor. MFI is the estimated modified Fournier index while the *R*-factor for the areas of Sicily and Morocco were also estimated in order to use the average of these values

Stations	Longitude easting	Latitude northing	Elevation (m)	Length of records (years)	Network	MFI	*R*-factor (Sicily)	*R*-factor (Morocco)	Mean *R*-factor
Askifou	516465.65	3905923.29	740	41	DHMA	317.72	4897.14	2548.48	3722.81
Vamos	517954.87	3918865.16	2	41	DHMA	127.82	1183.16	650.29	916.72
Chania	502820.04	3928089.54	62	52	DHMA	85.36	630.28	354.91	492.60
Kalybes	514922.29	3922556.43	24	27	DHMA	105.49	876.86	487.53	682.20
Mouri	510690.04	3899677.78	24	38	DHMA	150.45	1525.77	830.44	1178.10
PalaiaRoumata	480121.54	3917019.91	316	40	DHMA	200.75	2392.75	1279.97	1836.36
Palaioxora	470981.57	3898560.27	48	26	DHMA	90.98	696.11	390.49	543.30
Prasses	485373.58	3914557.69	520	10	DHMA	276.55	3943.73	2069.48	3006.61
Souda	510371.53	3933640.69	152	41	DHMA	88.63	668.36	375.50	521.93
Tavronitis	483599.79	3931737.57	15	35	NAGREF	98.56	788.75	440.33	614.54
ChaniaAgrokipio	504069.39	3927521.88	8	35	NAGREF	101.93	831.13	463.06	647.09
Drapanias	472990.90	3927381.61	29	19	NAGREF	109.32	927.06	514.34	720.70
Alikianos	491672.03	3923277.05		19	NAGREF	120.69	1081.77	596.62	839.20
Kandanos	476234.23	3908988.73	158	19	NAGREF	150.18	1521.53	828.22	1174.87
Koundoura	467145.75	3899182.45	59	9	NAGREF	72.49	488.44	277.75	383.10
Fragkokastello	520980.75	3892981.03		5	NAGREF	102.80	842.24	469.01	655.63
Falasarna	461634.71	3925886.21		12	NAGREF	94.88	743.26	415.89	579.58
Zymbragou	477729.91	3921328.00	235	19	NAGREF	155.51	1606.48	872.63	1239.56
Armenoi	514221.50	3920407.00	50	12	NAGREF	121.53	1093.62	602.90	848.26
Patsianos	521045.19	3895375.00		5	NAGREF	148.77	1499.21	816.53	1157.87
Anopolis	506878.00	3897748.00	600	12	IGME	135.78	1300.10	711.98	1006.04
Askyfou	516943.00	3905950.00	700	21	IGME	317.83	4899.77	2549.79	3724.78
Alikampos	519154.00	3911481.00	330	12	IGME	188.21	2163.75	1161.96	1662.85
Rodopou	477398.00	3934154.00	230	9	IGME	138.01	1333.60	729.61	1031.61
Epanoxori	484531.00	3908658.00	600	11	IGME	181.66	2047.41	1101.82	1574.61
Rogdia	467152.00	3915404.00	580	8	IGME	172.91	1895.65	1023.17	1459.41
Floria	475561.00	3914830.00	600	8	IGME	238.76	3136.05	1660.22	2398.14
Omalos	491146.00	3910915.00	1050	7	IGME	257.70	3532.60	1861.61	2697.10
Sirikari	466975.00	3919688.00	450	8	IGME	210.64	2579.21	1375.73	1977.47
Koystogerako	485010.00	3903952.00	530	12	IGME	164.36	1751.49	948.24	1349.87
Xasi (Boutas)	467500.00	3904906.00	370	14	IGME	122.97	1113.84	613.62	863.73
Prasses	486150.00	3914812.00	520	12	IGME	274.79	3904.66	2049.77	2977.21
Therissos	498286.00	3917629.00	580	21	IGME	194.51	2277.78	1220.78	1749.28
Melidoni	510334.00	3915922.00	400	21	IGME	198.40	2349.18	1257.55	1803.37
Kampoi	506136.00	3919063.00	560	12	IGME	211.71	2599.53	1386.16	1992.84

DHMA Department of Hydrology of the Ministry of Agriculture and Development Organization of Western Crete min, value; 383.10; *NAGREF* National Agricultural Research Foundation mean, value; 1429.41; *IGME* Institute of Geology and Mineral Exploration min, max, value; 3724.78

For this purpose, a simple range test and a spatial consistency test was applied to the data set. Daily reports queried by the quality testing were then simply dropped and no attempt was made to estimate appropriate replacements.

The rejection rate after the application of quality control was less than 0.5% for the data sets. Thus, there is no significant reduction in the data amount.

R-factor estimation

Based on the suggested methodology as reported earlier and using Eq. (3), the modified Fournier index (MFI) was estimated for all the rainfall gauges (Table 2, column 7). In order to estimate the most appropriate *R*-factor using the calculated MFI, the following two *R*–MFI relationships as suggested by the Ferro et al. (1999) and Renard and

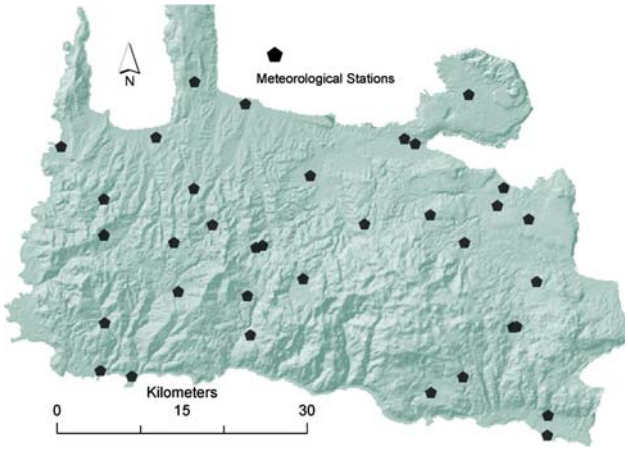

Fig. 2 Shaded relief map of the western Crete Island showing the location/spatial distribution of the meteorological (rain-gauges) stations used in the current research

Freimund (1994) for the regions of Sicily-Italy and the Morocco, respectively were used,

$$R = 0.6120 \cdot \mathrm{MFI}^{1.56}(\text{Sicily-Italy}) \quad (4)$$

$$R = 0.264 \cdot \mathrm{MFI}^{1.50}(\text{Morocco}) \quad (5)$$

The R factor for each of the relationships (4) and (5) was estimated, and the mean value of the resulted R factor was finally adopted as is shown in Table 2 (column 10).

In order to verify the reliability of the estimations, the calculated rainfall erosivity factors were interpolated with geostatistical as well as deterministic techniques. After applying and testing several geospatial prediction techniques the Ordinary Kriging interpolator was chosen for interpolating the point information (R factor). Compared with the remaining interpolation methods, it gave the best cross validation results and root mean squared (RMS) errors.

Table 3 presents the cross validation results of the estimated R factor. Cross-validation uses all of the data to estimate the trend. Then it omits each data location, one at a time, and predicts the associated data value. The predicted and actual values at the location of the omitted point are compared. For all points, cross-validation compares the measured and predicted values. For the standardized error estimation, the measured values are subtracted from the predicted values and then divided by the estimated standard errors. Generally, the best model is the one that has the mean nearest to zero and the smallest root-mean-squared prediction error. If the prediction errors are unbiased, the mean prediction error should be near zero but we should have always in mind that this value depends on the scale of the data.

Figure 3 shows the plot of the predicted versus the measured R factors. Details on the prediction errors, such as, the mean value (52.48), the root mean square (rms) (399), the average standard error (308.2), the mean standardized error (0.072) and the standardized rms (1.3) are given.

Soil erodibility factor (K)

The K factor is an empirical measure of soil erodibility as affected by intrinsic soil properties (Fu et al. 2006). The main soil properties affecting K are soil texture, organic matter, structure, and permeability of the soil profile.

Soil erodibility (K factor) was estimated with the help of the soil map provided by the Soil Geographical Data Base of Europe at a scale of 1:1,000,000 which is available online on http://eusoils.jrc.it/. This map makes a distinction among coarse (<18% clay and >65% sand), medium (18–35% clay and ≥15% sand, or 18% < clay and 15–65% sand), medium fine (<35% clay and <15% sand), fine (35–60% clay) and very fine (clay >60%) soil texture types.

After comparison between the geological maps of the Chania Prefecture and the soil types on the available soil map we proceeded to the in situ check of soil samples for any geological formation which was included in each one of the four polygonal areas (i.e. soil types) of the Soil Geographical Data Base of Europe at Scale 1:1,000,000. Afterwards, the K factor was calculated by means of the following formulae which were developed from global data of measured K values, obtained from 225 soil classes (Renard et al. 1997):

$$K = 0.0034 + 0.0405 \times \exp\left[-0.5\left(\frac{\log D_g + 1.659}{0.7101}\right)^2\right] \quad (6)$$

$$D_g = \exp\left(\sum f_i \ln\left(\frac{d_i + d_{i-1}}{2}\right)\right) \quad (7)$$

where D_g is the geometric mean particle size, for each particle size class (clay, silt, sand), d_I is the maximum diameter (mm), d_{I-1} is the minimum diameter and f_I is the corresponding mass fraction.

This relation is very useful with soils for which data are limited and/or the textural composition is given in a particular classification system.

Slope-length (L) and slope steepness (S) factors

The L and S factors in RUSLE reflect the effect of topography on erosion. It has been demonstrated that increases in slope length and slope steepness can produce higher overland flow velocities and correspondingly higher erosion (Haan et al. 1994). Moreover, gross soil loss is considerably more sensitive to changes in slope steepness than to changes in slope length (McCool et al. 1987). Slope length has been broadly defined as the distance from the

Table 3 Cross-validation results of the estimated *R*-factor

Stations	Estimated *R*-factor	Predicted *R*-factor	Error (%)	Standard error	Standardized error
Askifou	3722.8	3491.9	6.2	177.4	−1.3
Vamos	916.7	770.1	16.0	326.0	−0.4
Chania	492.6	553.6	12.4	253.2	0.2
Kalybes	682.2	598.7	12.2	291.2	−0.3
Mouri	1178.1	704.8	40.2	324.6	−1.5
PalaiaRoumata	1836.4	1692.1	7.9	310.4	−0.5
Palaioxora	543.3	12.1	97.8	333.1	−1.6
Prasses	3006.6	2592.8	13.8	185.2	−2.2
Souda	521.9	1025.9	96.6	350.2	1.4
Tavronitis	614.5	462.4	24.8	334.7	−0.5
ChaniaAgrokipio	647.1	426.4	34.1	250.9	−0.9
Drapanias	720.7	739.7	2.6	334.5	0.1
Alikianos	839.2	872.8	4.0	333.1	0.1
Kandanos	1174.9	815.5	30.6	324.7	−1.1
Koundoura	383.1	187.7	51.0	336.7	−0.6
Fragkokastello	655.6	681.4	3.9	314.3	0.1
Falasarna	579.6	493.6	14.8	349.0	−0.2
Zymbragou	1239.6	1372.9	10.8	323.8	0.4
Armenoi	848.3	790.7	6.8	272.2	−0.2
Patsianos	1157.9	654.8	43.4	306.2	−1.6
Anopolis	1006.0	2158.6	114.6	330.3	3.5
Askyfou	3724.8	3506.6	5.9	177.0	−1.2
Alikampos	1662.9	1985.0	19.4	331.3	1.0
Rodopou	1031.6	1248.4	21.0	338.1	0.6
Epanoxori	1574.6	2323.9	47.6	314.5	2.4
Rogdia	1459.4	2152.6	47.5	329.4	2.1
Floria	2398.1	2308.3	3.7	318.8	−0.3
Omalos	2697.1	3603.9	33.6	328.8	2.8
Sirikari	1977.5	1752.0	11.4	324.3	−0.7
Koystogerako	1349.9	1734.8	28.5	325.9	1.2
Xasi (Boutas)	863.7	1248.6	44.6	336.6	1.1
Prasses	2977.2	2720.6	8.6	192.0	−1.3
Therissos	1749.3	1808.2	3.4	331.8	0.2
Melidoni	1803.4	1972.2	9.4	319.9	0.5
Kampoi	1992.8	2402.1	20.5	321.6	1.3

point of origin of overland flow to the point where either the slope gradient decreases enough where deposition begins or the flow is concentrated in a defined channel (Wischmeier and Smith 1978). The specific effects of topography on soil erosion are estimated by the dimensionless *LS* factor as the product of the slope length (*L*) and slope steepness (*S*) constituents converging onto a point of interest, such as a farm field or a cell on a GIS raster grid.

In the current work, the digital elevation model (DEM) of the study area with a cell size of 20 m was used for the calculation of the *LS* factor. There are many formulas capable of calculating the *L* and *S* factors. In the new array-based framework that has been adopted, the overall flow path-based iterative slope-length accumulation and *LS* factor computation steps were performed inside Arc-Info Grid using the RUSLE Version 4 (an AML) (Van Remortel et al. 2001). As a result, each 20 m cell of the grid surface of each one of the watersheds was assigned an *LS* value.

Cover Management factor (*C*)

The vegetation cover and management factor *C* represent the effect of cropping and management practices in agricultural management, and the effect of ground, tree, and grass covers on reducing soil loss in non-agricultural

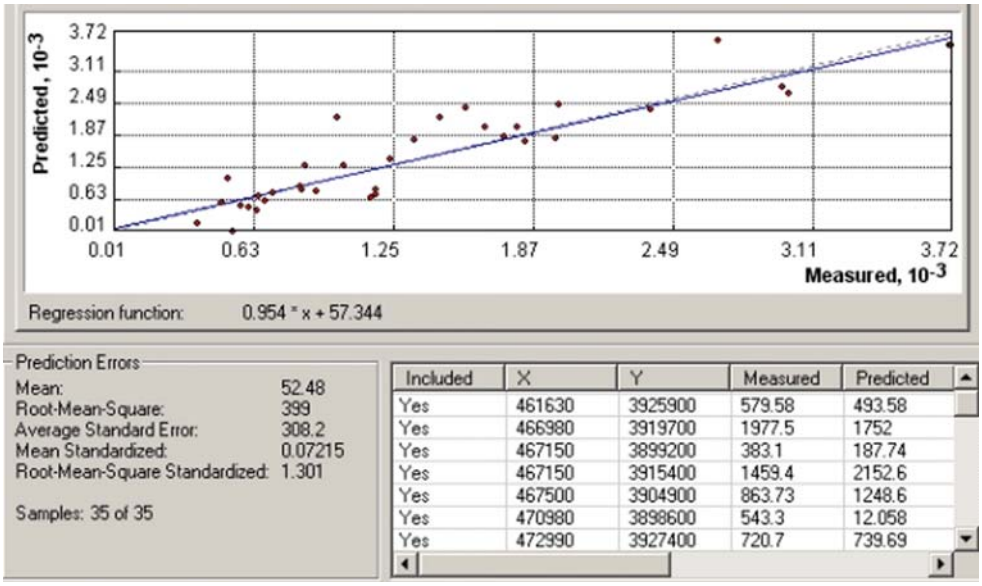

Fig. 3 Geostatistical analysis of the resulted parameters applying cross validation control on the estimated *R*-factor

situation. As the vegetation cover increases, the soil loss decreases. According to Benkobi et al. (1994) and Biesemans et al. (2000), the vegetation cover factor together with slope steepness and length factors is most sensitive to soil loss. In the USLE, the vegetation cover *C* factor is derived based on empirical equations with measurements of ground cover, aerial cover, and minimum drip height (Wischmeier and Smith 1978).

The most widely used remote-sensing derived indicator of vegetation growth is the Normalized Difference Vegetation Index, which for Landsat-ETM is given by the following equation:

$$\mathrm{NDVI} = \frac{L_{\mathrm{TM4}} - L_{\mathrm{TM3}}}{L_{\mathrm{TM4}} + L_{\mathrm{TM3}}} \tag{8}$$

This index is an indicator of the energy reflected by the Earth related to various cover type conditions. NDVI values range between −1.0 and +1.0. When the measured spectral response of the earth surface is very similar to both bands, the NDVI values will approach zero. A large difference between the two bands results in NDVI values at the extremes of the data range.

Photosynthetically active vegetation presents a high reflectance in the near IR portion of the spectrum (Band 4,

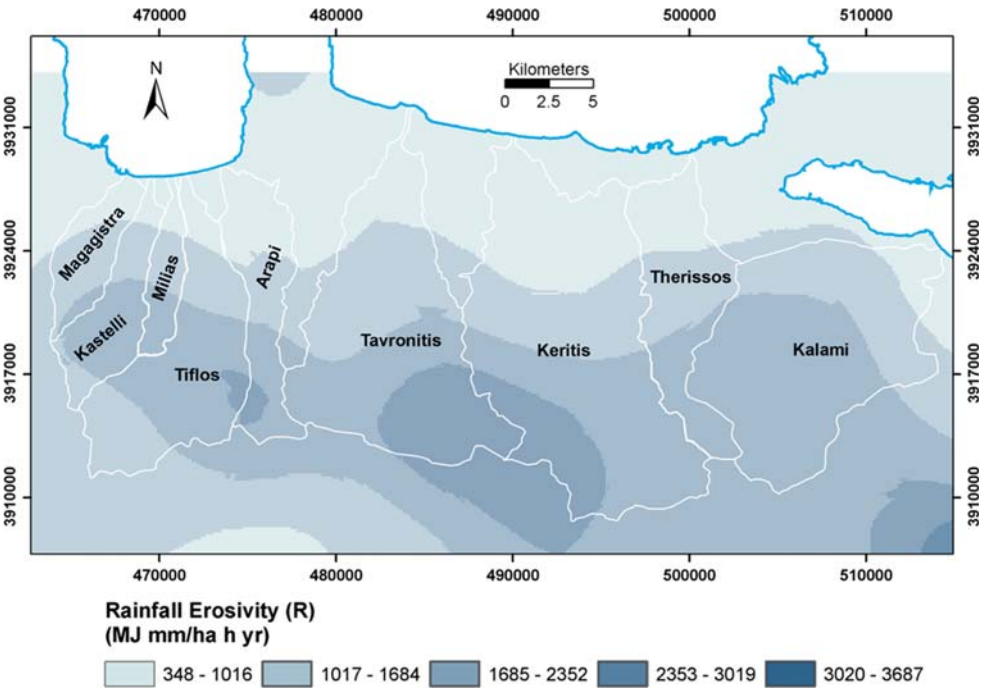

Fig. 4 Grid surface of the western Crete Island showing the spatial distribution of the calculated *R*-factor

Table 4 Statistical data of the *R*-factor for each watershed

Watersheds	Number of pixels	Min *R*-factor	Max *R*-factor	Mean *R*-factor
Keritis	448,016	712.0	2887.2	1799.6
Tavronitis	326,720	580.0	2958.7	1769.4
Kastelli	79,254	745.0	2038.0	1391.5
Tiflos	190,159	697.5	2452.7	1575.1
Arapi	103,766	692.8	2446.7	1569.8
Therissos	143,660	522.0	1930.9	1226.4
Magagistra	56,305	767.6	1844.8	1306.2
Milias	38,370	702.9	2066.1	1384.5
Kalami	32,4023	676.3	2163.2	1419.8

Table 5 Statistical data of the *LS*-factor for each watershed in the study area

Watersheds	Min	Max	Mean	Std
Milias	nz	45	5.58	5.35
Arapi	nz	66	6.28	6.84
Magagistra	nz	71	6.55	7.47
Therissos	nz	78	6.74	8.29
Kalami	nz	118	7.63	9.54
Tiflos	nz	84	8.16	7.81
Kastelli	nz	110	8.97	8.84
Keritis	nz	113	9.14	10.25
Tavronitis	nz	98	9.78	9.11

nz near zero

Landsat TM), in comparison with the visible portion (red, Band 3, Landsat TM); therefore, NDVI values for photosynthetically active vegetation will be positive. Areas with or without low vegetative cover (such as bare soil, urban areas), as well as inactive vegetation (unhealthy plants) will usually display NDVI values fluctuating between −0.1 and +0.1. Clouds and water bodies will give negative or zero values.

A scene of Landsat ETM images acquired on 30 June 2000 with a spatial resolution of 30 m was used. These images consisted of band 1: 0.45–0.53 mm, band 2: 0.52–0.60 mm, band 3: 0.63–0.69 mm, band 4: 0.76–0.90 mm, band 5: 1.55–1.75 mm, and band 7: 2.08–2.35 mm. The snow area of the image was masked and the NDVI image was then produced. After the production of the NDVI image, the following formula was used to generate a *C* factor surface from NDVI values (Van der Knijff et al. 1999, 2000; Van Leeuwen and Sammons 2004):

$$C = e^{(-\alpha((\mathrm{NDVI})/(\beta-\mathrm{NDVI})))} \quad (9)$$

where α and β are unitless parameters that determine the shape of the curve relating to NDVI and the *C* factor.

Van der Knijff et al. (1999, 2000) found that this scaling approach gave better results than assuming a linear relationship. Finally, the values of 2 and 1 was selected for the parameters α and β, respectively, since the resulted values were in a good agreement with the values mentioned in the related literature and had the best correlation with the

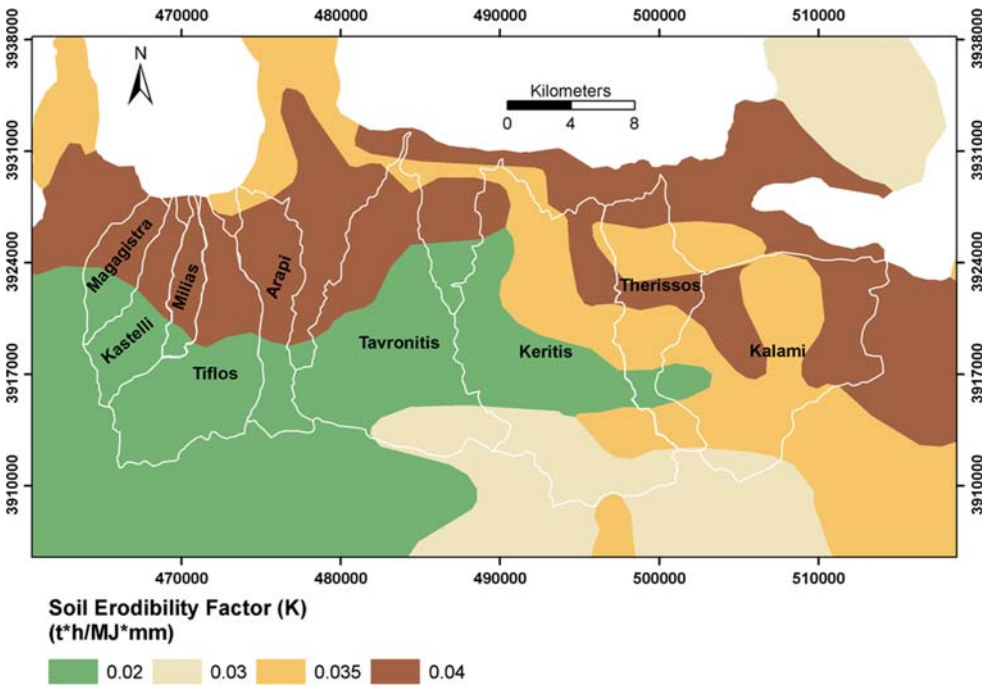

Fig. 5 The Soil Erodibility Factor (*K*) map of the study area

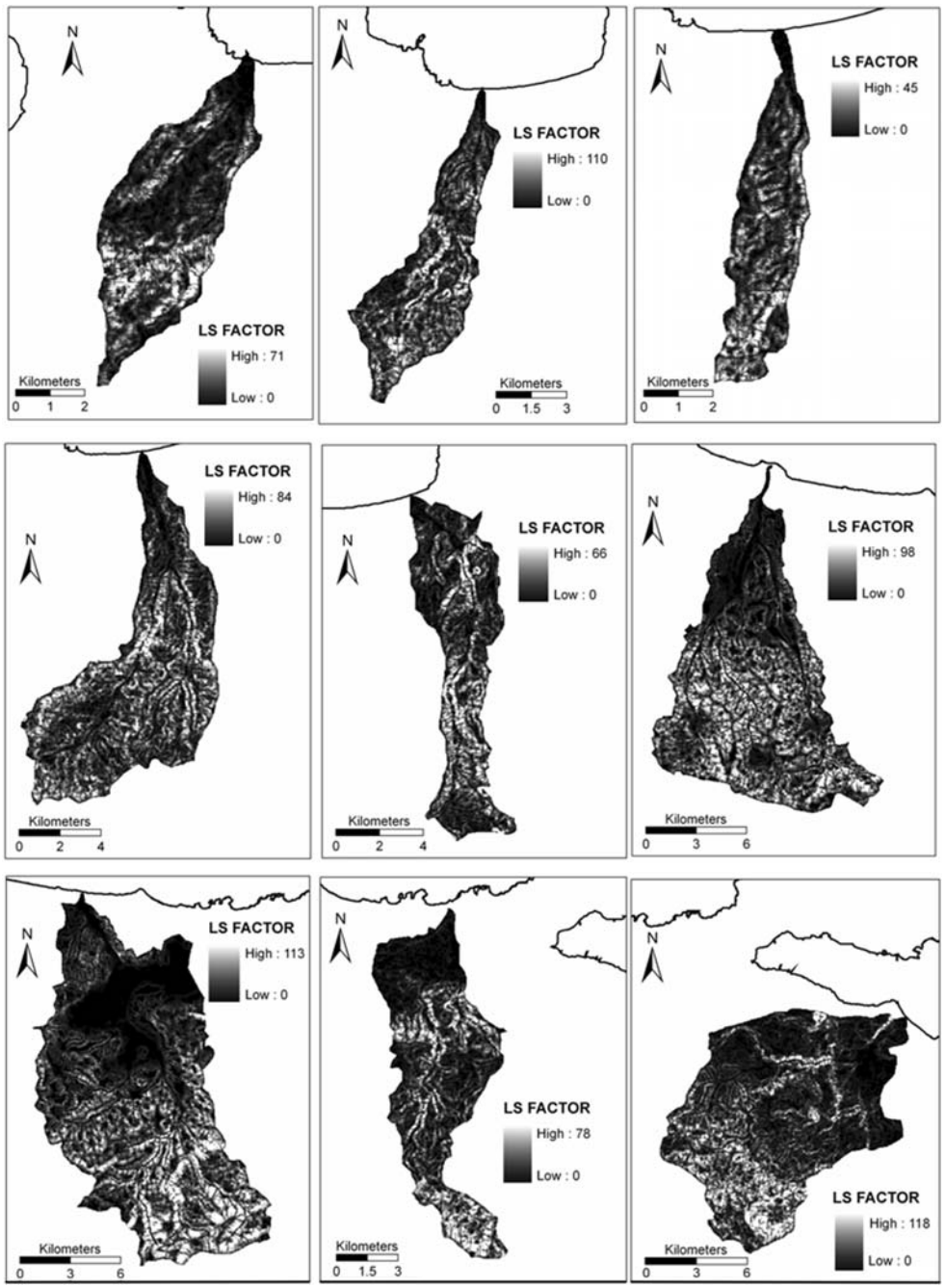

Fig. 6 The LS maps for the nine watersheds

Corine Land Cover map 2000 (CLC2000 100 m, version 1) of the European Environment Agency (©EEA, Copenhagen, 2000; http://www.eea.europa.eu). This map has a resolution of 100 m and uses 18 land use categories for the study area from a total of 44 land uses of level 3. As the *C* factor ranges between 0 and 1, a value of 0 was assigned to a few pixels with negative values and a value of 1 to pixels with value greater than 1.

Results and discussion

Rainfall erosivity factor

By using the values of the *R* factor estimated for each investigated rain-gauge (35 meteo-stations in western Crete) and a kriging interpolation method, the isoerosivity map of the study area is produced as is shown in Fig. 4.

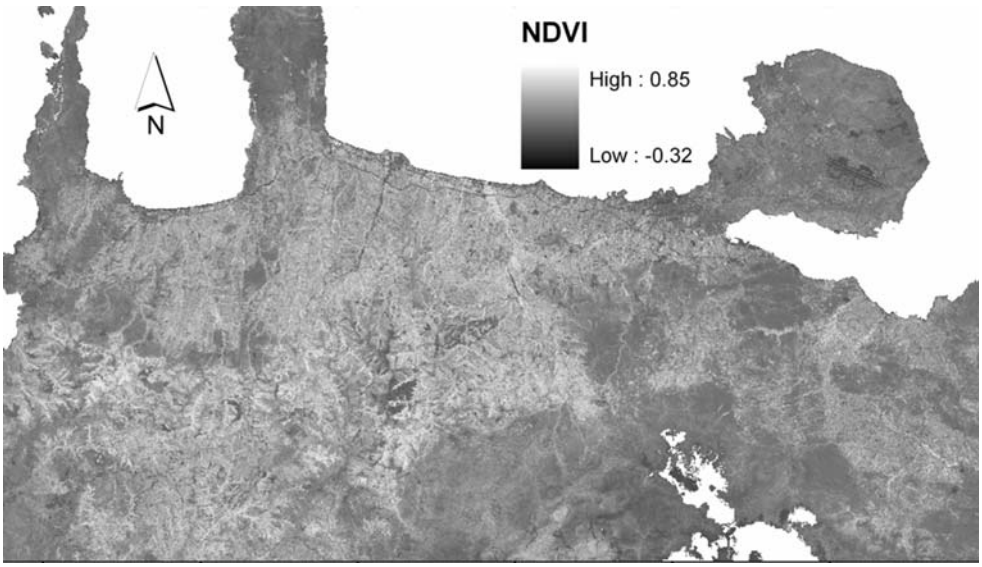

Fig. 7 The NDVI thematic map resulted from the Landsat-ETM satellite image of the study area showing a range from −0.32 to 0.85

The mean values of the *R* factor range from 1226.4 MJ mm/ha year^{-1} for the Therisso watershed to 1799.6 MJ mm /ha year^{-1} for Keritis watershed. The calculated *R* factors were subdivided into five classes showing high erosivity (3020–3687 MJ mm /ha year^{-1}) in the broader area of White Mountains. Medium to high erosivity (2353–3019 MJ mm /ha year^{-1}) in the southern part of Keritis and Tavronitis watersheds is observed which is in agreement with the results of Kouli et al. (2007). As the topography changes going from steep (mountainous areas) to flat relief (coastal areas) the erosivity decreases normally from 2,352 to 348 MJ mm/ha year^{-1}. Moreover, some statistical information for the investigated watersheds are given in Table 4 concerning the number of pixels and the minimum, maximum, and average *R* factor value for each one of the nine watersheds of the northwestern Crete Island.

Soil erodibility factor

The *K* factor for each sample was calculated considering mean values of grain size. Soil erodibility values range

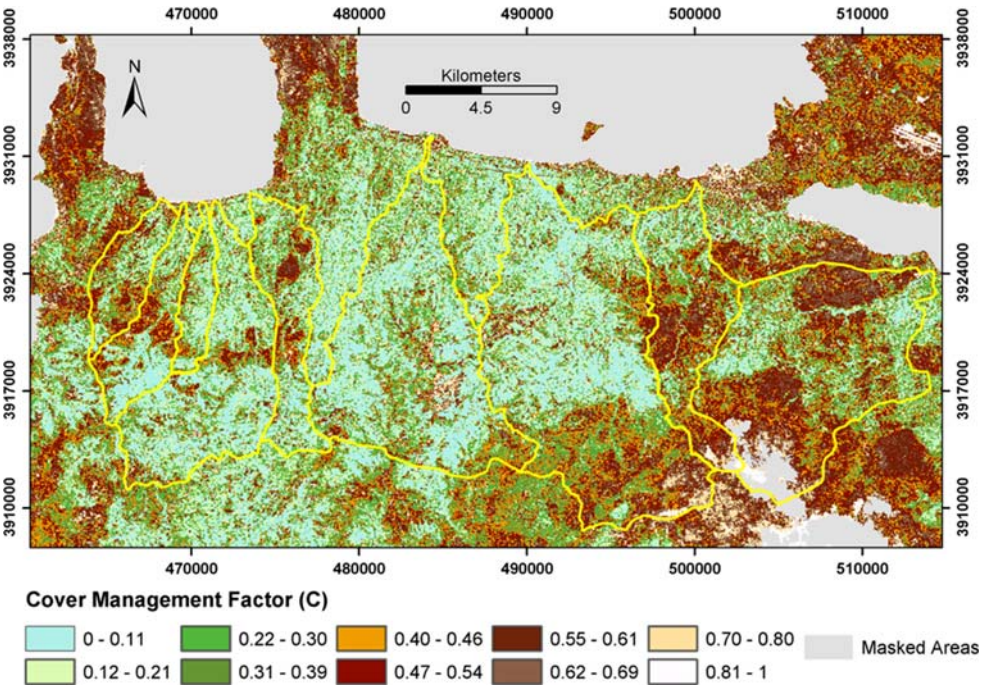

Fig. 8 The cover management factor distribution which derived from the NDVI image (Fig. 7)

Table 6 The average *C* factor values for the several land uses of the study area

Land use	Mean
Broad-leaved forest	0.130266
Fruit trees and berry plantations	0.178411
Mixed forest	0.182351
Vineyards	0.294141
Olive groves	0.304188
Land principally occupied by agriculture	0.307676
Coniferous forest	0.338087
Transitional woodland—shrub	0.375549
Sclerophyllous vegetation	0.412805
Complex cultivation patterns	0.428191
Non-irrigated arable land	0.496456
Moors and heathland	0.500111
Pastures	0.543197
Natural grasslands	0.545464
Construction sites	0.548493
Beaches, dunes, sands	0.575484
Sparsely vegetated areas	0.644916
Bare rocks	0.785093

from 0.02 t ha MJ^{-1} mm^{-1} in large areas in the western part of the study area (sandy soils) to 0.03, 0.035 and 0.04 t ha MJ^{-1} mm^{-1} for the loamy and silt loamy soils, in the southern and central parts of the study area, respectively (Fig. 5). The highest values of the soil erodibility factor are spatially well correlated with the areas which expose quaternary and neogene sediments.

LS factor

The Kalami watershed shows the greatest *LS* factor among the nine studied watersheds (Table 5). The topographic factor ranges from 0 in the flat zones to 118 at the steep slopes in the southern part of the basin. Although Kalami basin is characterized by the greatest elevation drop of 2,187 m and consequently the greatest *LS* factor, the great values are present in a limited part of the basin (Fig. 6). On the other hand, Tavronitis, Keritis and Kastelli watersheds show *LS* factor equal to 98, 113 and 110, respectively, but the mean values are far greater than that of Kalami basin (Fig. 6). This fact implies that extended areas of steep slopes are prone to severe erosion. On the other hand, Milias watershed is characterized by relatively small *LS* factor values and this is consistent with the low elevation values (20 to 816 m) and the smallest extent of the watershed (Fig. 6). The fact that despite its relatively low elevation the Kastelli basin (20 to 1,061 m) has high maximum and mean *LS* factor values of 110 and 8.97 is noteworthy.

Cover management factor

The NDVI thematic map resulted from the Landsat-ETM satellite image of the study area showing a range from −0.32 to 0.85 (Fig. 7). The Corine Land Cover vector map was overlain to the pixel by pixel estimated cover management factor grid (Fig. 8) and the mean *C* value for every Corine class was calculated (Table 6). As a result, the mean *C* values range inside the watersheds from 0.13 for the forest class to 0.785 for the bare rocks class (Table 6). The *C* values for forest are near 0 and for the bare rocks tending to 1 which looks realistic. The predicted *C* values of the arable classes depend on crop type and management practices.

The approach followed here was based on the available data. To improve the results, satellite images with better geometric and spectral characteristics can provide detailed information, as well as field measurements can be proved efficient to relate biophysical properties (like the *C* factor) to remotely-sensed data. (Fig. 9)

Soil loss

Soil loss values were computed by overlaying four grid surfaces of the nine catchments: the grid surface representing the *R* factor values, the grid surface representing the *K* factor values, the grid surface representing the *C* factor values, and the grid surface representing the *LS* factor values.

Soil loss values (Table 7) range between 0 and 1982 t/ha $year^{-1}$ for the Magagistra watershed, with a mean value of 85,513 t/ha $year^{-1}$, between 0 and 3975 t/ha $year^{-1}$ with a mean value of 107.625 t/ha $year^{-1}$ for the Kastelli watershed, between 0 and 1,150 t/ha $year^{-1}$ for Milias basin with a mean value of 77.174 t/ha $year^{-1}$, between 0 and 3901 t/ha $year^{-1}$ for the Tiflos basin (mean value equal to 82.666 t/ha $year^{-1}$), between 0 and 2366 t/ha $year^{-1}$ for the Arapi watershed (mean value equal to 83.725 t/ha $year^{-1}$), between 0 and 3733 t/ha $year^{-1}$ for the Tavronitis basin with a mean value of 125.69 t/ha $year^{-1}$, between 0 and 4254 t/ha $year^{-1}$ for the Keritis watershed (mean value equal to 193.527 t/ha $year^{-1}$) and between 0 and 4156 t/ha $year^{-1}$ for the Kalami watershed with a mean value of 205.467 t/ha $year^{-1}$. The highest soil loss values are spatially correlated with the steepest slopes.

Conclusions

The RUSLE model was applied to estimate soil loss in the nine major watersheds of the northwestern part of Crete Island. Detailed data for the computation of the *R*-, *K*- and

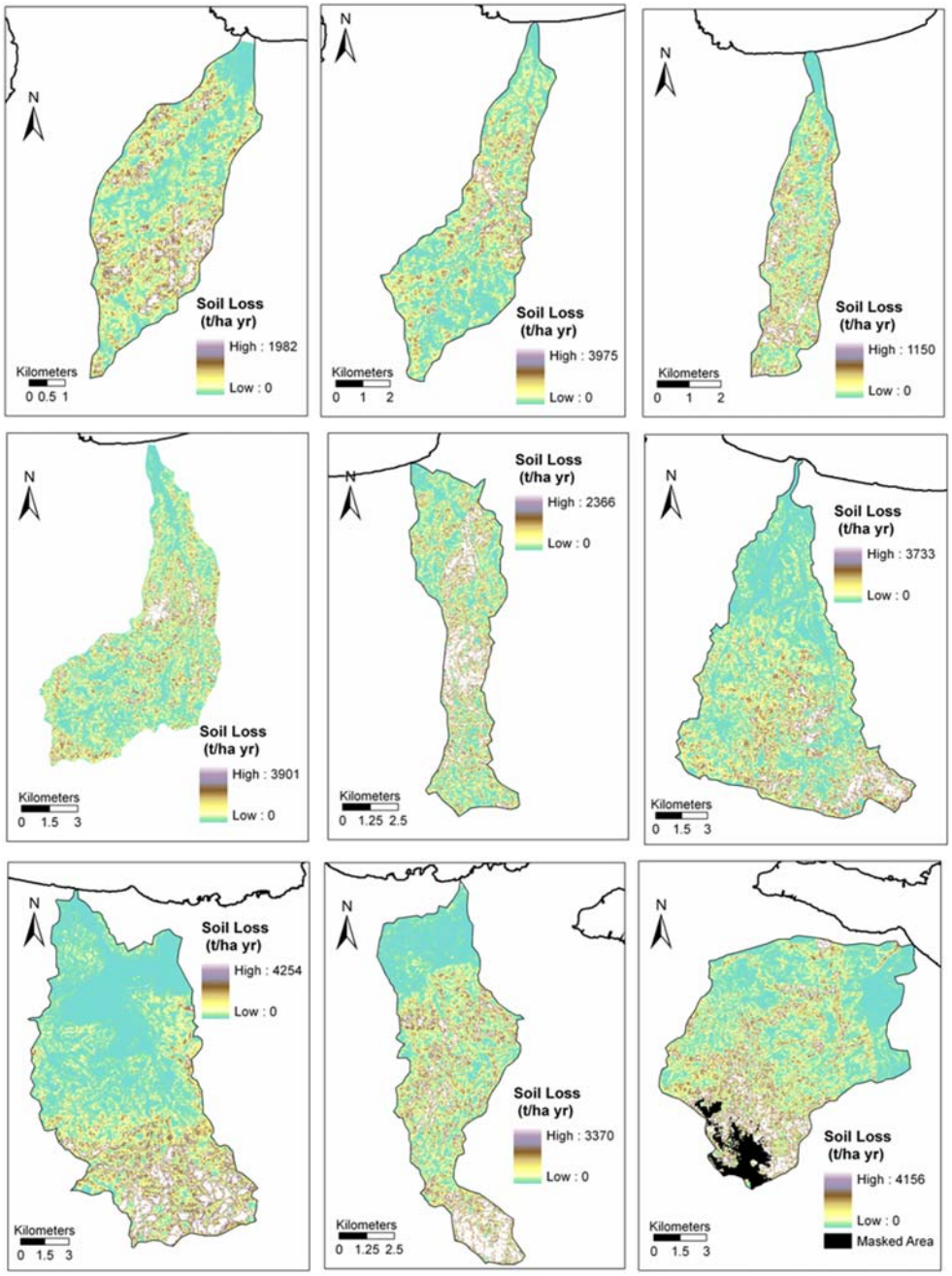

Fig. 9 Soil loss maps for each watershed (from west to east), after the application of the RUSLE equation

C- factors were not available; therefore these parameters were estimated either by means of general or approximation formulae or by processing available satellite images (i.e. for the extraction of the cover management, *C* factor). Moreover, the estimation of *LS* factor was performed with the use of a GIS automated technique to generate slope length and slope steepness.

The results of the application of the RUSLE model seem to be consistent with those obtained for other Mediterranean watersheds of similar characteristics.

However, we must note the complete lack of data for the estimation of *P* factor, which was set to 1. The current study shows that even if some uncertainties are present, the RUSLE model can be efficiently applied at the basin scale with quite modest data requirements in a typical Mediterranean environment such as the investigated river basins. Further analysis of the *P* factor could improve the results. However, the obtained results are still very important as they quantify the soil loss and point the water basins which are exposed to great danger of soil erosion, a serious

Table 7 The minimum, maximum and mean soil loss values for the nine watersheds of the northern part of Chania Prefecture

Watersheds	Min. soil loss (t/ha year^{-1})	Max. soil loss (t/ha year^{-1})	Mean soil loss (t/ha year^{-1})
Milias	nz	1,150	77.174
Tiflos	nz	3,901	82.666
Arapi	nz	2,366	83.725
Magagistra	nz	1,982	85.513
Kastelli	nz	3,975	107.625
Tavronitis	nz	3,733	125.691
Therissos	nz	3,370	163.217
Keritis	nz	4,254	193.527
Kalami	nz	4,156	205.467

nz near zero

problem in the island of Crete, the biggest Greek island with great agricultural activity.

Acknowledgments The project is co-funded by the European Social Fund and National Resources in the framework of the project INTERREG III B ARCHIMED, sub-project A1.020 entitled "MILDMAP—Methodology Integration of EO techniques as operative tool for Land Degradation Management and planning in Mediterranean Areas". The authors are grateful to the anonymous reviewers for their very helpful comments and valuable suggestions.

References

Arnoldus HMJ (1980) An approximation of the rainfall factor in the Universal Soil Loss Equation. In: De Boodt M, Gabriels D (eds) Assessment of erosion. Wiley, Chichester, pp 127–132

Aronica G, Ferro V (1997) Rainfall erosivity over Calabrian region. Hydrol Sci J 42(1):35–48

Bagarello V (1994) Procedure semplificate per la stima del fattore climatico délia USLE nelPambiente molisano (Simplified procedures for estimating the climatic factor of the USLE in Molise, in Italian). Atti delta Giornata di Studio Sviluppi Recenti delle Ricerche sull'Ewsione e sul suo Controllo, Bari, 17–18 February 1994

Banasik K, Gôrski D (1994) Rainfall erosivity for South-East Poland. In: Rickson RJ (ed) Conserving soil resources. European perspectives. Lectures in soil erosion control, Silsoe College, Cranfield University, UK, pp 201–207

Benkobi L, Trlica MJ, Smith JL (1994) Evaluation of a refined surface cover subfactor for use in RUSLE. J Range Manage 47:74–78

Bergsma E (1980) Provisional rain-erosivity map of The Netherlands. In: De Boodt M, Gabriels D (eds) Assessment of erosion. Wiley, Chichester

Biesemans J, Meirvenne MV, Gabriels D (2000) Extending the RUSLE with the Monte Carlo error propagation technique to predict long-term average off-site sediment accumulation. J Soil Water Conserv 55:35–42

Bolinne A, Laurant A, Rosseau P (1980) Provisional rain-erosivity map of Belgium. In: De Boodt M, Gabriels D (eds) Assessment of erosion. Wiley, Chichester, pp 111–120

Boyle M (2002) Erosion's contribution to greenhouse gases. Erosion Control 9:64–67

Brown LR (1984) Conserving soils. In: Brown LR (ed) State of the world. Norton, New York, pp 53–75

Chartzoulakis KS, Paranychianakis NV, Angelakis AN (2001) Water resources management in the island of Crete, Greece, with emphasis on the agricultural use. Water Policy 3:193–205

Cox C, Madramootoo C (1998) Application of Geographic Information Systems in watershed management planning in St. Lucia. Comput Electron Agric 20:229–250

Erdogan EH, Erpul G, Bayramin I (2007) Use of USLE/GIS methodology for predicting soil loss in a semiarid agricultural environment. Environ Monit Assess 131:153–161

Fernandez C, Wu JQ, McCool DK, Stockle CO (2003) Estimating water erosion and sediment yield with GIS, RUSLE,and SEDD. J Soil Water Conserv 58:128–136

Ferro V, Giordano G, Lovino M (1991) Isoerosivity and erosion risk map for Sicily. Hydrol Sci J 36(6):549–564

Ferro V, Porto P, Yu B (1999) A comparative study of rainfall erosivity estimation for Southern Italy and southeastern Australia. Hydrol Sci J Sci Hydrol 44(1):3–24

Fu G, Chen S, McCool KD (2006) Modeling the impacts of no-till practice on soil erosion and sediment yield using RUSLE, SEDD and ArcView GIS. Soil Tillage Res 85:38–49

Gabriels D, Cadron W, De Mey P (1986) Provisional rain erosivity maps of some EC countries. In: Proc. workshop on erosion assessment and modeling, Brussels, Belgium

Gong J (2001) Geography information system. Science Publishing, Beijing

Haan CT, Barfield BJ, Hayes JC (1994) Design hydrology and sedimentology for small catchments. Academic Press, San Diego, 588pp

Hussein MH (1986) Rainfall erosivity in Iraq. J Soil Water Conserv 41:336–338

Kouli M, Vallianatos F, Soupios P, Alexakis D (2007) A GIS example of morphometric analysis in two major watersheds of Western Crete, Greece. J Environ Hydrol 15(1):1–17

Krahl J, Kauffmann G, Kozur H, Richter D, Forster O, Heinritzi F (1983) Neue Daten zur Biostratigraphie und zur tektonischen Lagerung der Phyllit-Gruppe und der Trypali-Gruppe aufder Insel Kreta (Griechenland). Geol Rundsch 72:1147–1166

Lal R (1990) Soil erosion in the tropics: principles and management. McGraw-Hill, New York

Lal R (1994) Soil erosion by wind and water: problems and prospects. In: Lal R (ed) Soil erosion research methods, 2nd edn. Soil and Water Conservation Society, St. Lucie Press, America pp 1–9

Lal R (2001) Soil conservation for C sequestration. In: Stott DE, Mohtar RH, Steinhardt GC (eds) Proceedings of the 10th international soil conservation organization meeting, 24–29 May 1999, West Lafayette, pp 459–465

Lewis LA, Verstraeten G, Zhu H (2005) RUSLE applied in a GIS framework: calculating the LS factor and deriving homogeneous patches for estimating soil loss. Int J Geogr Inf Sci 19(7):809–829

Lim KJ, Sagong M, Engel BA, Tang Z, Choi J, Kim KS (2005) GIS-based sediment assessment tool Catena 64:61–80

Lo A, El-Swaify SA, Dangler EW, Shinshiro L (1985) Effectiveness of EI30 as an erosivity index in Hawaii. In: El-Swaify SA, Moldenhauer WC, Lo A (eds) So/7 erosion and conservation. Soil Conservation Society of America, Ankeny, pp 384–392

McCool DK, Brown LC, Foster GR (1987) Revised slope steepness factor for the universal soil loss equation. Trans Am Soc Agric Eng 30:1387–1396

Mikhailova EA, Bryant RB, Schwager SJ, Smith SD (1997) Predicting rainfall erosivity in Honduras. Soil Sci Soc Am J 61:273–279

Millward AA, Mersey JE (1999) Adapting the RUSLE to model soil erosion potential in a mountainous tropical watershed. Catena 38:109–129

Mitasova H, Hofierka J, Zlocha M, Iverson LR (1996) Modeling topographic potential for erosion and deposition using GIS. Int J GIS 10:629–642

Mitsios J, Pashalidis C, Panagias K (1995) Soil erosion—mitigation techniques to soil erosion. Zymel Editions, Athens

Molnar DK, Julien PY (1998) Estimation of upland erosion using GIS. Comput Geosci 24:183–192

Morgan RPC (1992) Soil erosion in the northern countries of the European Community. EIW Workshop: elaboration of a framework of a code of good agricultural practices, Brussels, 21–22 May 1992

Nyakatawa EZ, Reddy KC, Lemunyon JL (2001) Predicting soil erosion in conservation tillage cotton production systems using the revised universal soil loss equation. Soil Till Res 57:213–224

Oldeman LR, Hakkeling RTA, Sombroek WG (1991) World map of the status of human-induced soil degradation, with explanatory note (second revised edition)—ISRIC, Wageningen; UNEP, Nairobi

Onori F, De Bonis P, Grauso S (2006) Soil erosion prediction at the basin scale using the revised universal soil loss equation (RUSLE) in a catchment of Sicily (southern Italy). Environ Geol 50:1129–1140

Ouyang D, Bartholic J (1997) Predicting sediment delivery ratio in Saginaw Bay watershed. In: Proceedings of the 22nd National Association of Environmental Professionals Conference, 19–23 May 1997, Orlando, FL, pp 659–671

Renard KG, Foster GR (1983) Soil conservation: principles of erosion by water. In: Dregne HE, Willis WO (eds) Dryland agriculture. Agronomy Monograph No. 23. American Society of Agronomy, Crop Science Society of America, and Soil Science Society of America, Madison, pp 155–176

Renard KG, Freimund JR (1994) Using monthly precipitation data to estimate the *R* factor in the revised USLE. J Hydrol 157:287–306

Renard KG, Foster GR, Weesies GA, McCool DK (1996) Predicting soil erosion by water. A guide to conservation planning with the revised universal soil loss equation (RUSLE). Agric. Handbook 703. US Govt Print Office, Washington, DC

Renard KG, Foster GR, Weesies GA, McCool DK, Yoder DC (1997) Predicting soil erosion by water: a guide to conservation planning with the Revised Universal Soil Loss Equation (RUSLE). Agriculture Handbook No. 703, USDA-ARS

Stocking MA, Elwell HA (1973) Prediction of sub-tropical storm soil losses from field plot studies. Agric Meteorol 12:193–201

Tsagarakis KP, Dialynas GE, Angelakis AN (2004) Water resources management in Crete (Greece) including water recycling and reuse and proposed quality criteria. Agric Water Manage 66:35–47

Van der Knijff M, Jones RJA, Montanarella L (1999) Soil erosion risk in Italy. EUR19022 EN. Office for Official Publications of the European Communities, Luxembourg, 54p

Van der Knijff JM, Jones RJA, Montanarella L (2000) Soil erosion risk assessment in Europe. EUR 19044 EN. Office for Official Publications of the European Communities, Luxembourg, 34p

Van Leeuwen WJD, Sammons G (2004) Vegetation dynamics and soil erosion modeling using remotely sensed data (MODIS) and GIS. Tenth Biennial USDA Forest Service Remote Sensing Applications Conference, 5–9 April 2004, Salt Lake City, UT. US Department of Agriculture Forest Service Remote Sensing Applications Center, Salt Lake City:

Van Lynden GWJ (1995) European soil resources. Nature and environment No.71. Council of Europe, Strasbourg

Van Remortel RD, Hamilton ME, Hickey RJ (2001) Estimating the LS factor for RUSLE through iterative slope length processing of digital elevation data within ArcInfo Grid. Cartography 30(1):27–35

Wischmeier WH (1959) A rainfall erosion index for a universal soil-loss equation. Soil Sci Soc Am Proc 23:246–249

Wischmeier WH, Smith DD (1965) Predicting rainfall-erosion losses from ropland east of the Rocky Mountains. Guide for selection of practices for soil and water conservation. Agric. Handbook, 282. US Gov. Print. Office, Washington, DC

Wischmeier WH, Smith DD (1978) Predicting rainfall erosion losses—a guide to conservation planning. Agriculture Handbook No. 537. US Department of Agriculture Science and Education Administration, Washington, DC, USA, 163 pp

Wu Q, Dong D (2001) GIS based theories and methods for investigations of geological hazard and water resources. Geology Publishing Company, Beijing

Wu Q, Wang M (2007) A framework for risk assessment on soil erosion by water using an integrated and systematic approach. doi:10.1016/j.jhydrol.2007.01.022

Yitayew M, Pokrzywka SJ, Renard KG (1999) Using GIS for facilitating erosion estimation. Appl Eng Agric 15:295–301

Yoder D, Lown J (1995) The Future of RUSLE: inside the new revised universal soil loss equation. J Soil Water Conserv 50(5):484–489

Yu B, Rosewell CJ (1996a) An assessment of a daily rainfall erosivity model for New South Wales. Aust J Soil Res 34:139–152

Yu B, Rosewell CJ (1996b) Rainfall erosivity estimation using daily rainfall amounts for South Australia. Aust J Soil Res 34:721–733

Yu B, Rosewell CJ (1996c) A robust estimator of the *R* factor for the Universal Soil Loss Equation. Trans Am Soc Agric Eng 39(2):559–561